Extension and validation of a geographic information system–based method for calculating the Revised Universal Soil Loss Equation length-slope factor for erosion risk assessments in large watersheds

M.F. Winchell, S.H. Jackson, A.M. Wadley, and R. Srinivasan

Abstract: A geographic information system-based (GIS) method for estimating the length-slope (*LS*) factor of the Revised Universal Soil Loss Equation using national-scale datasets was developed and validated. The method was applied to approximately two-thirds of the Mississippi River basin, focusing on agricultural subwatersheds in the Midwest. The results were validated by comparing the GIS-based statistical distributions of *LS*-factor values with the distribution of *LS*-factors calculated from the Natural Resources Inventory database at the eight-digit watershed level. The GIS-based approach was shown to produce statistical distributions of *LS*-factor values very similar to those described by the Natural Resources Inventory database of field measurements, providing for the first time strong support for using GIS-based methods to represent the spatial heterogeneity and magnitude of *LS*-factors. Development and validation of the GIS-based approach is an important step toward conducting large-scale erosion potential assessments that have soil conservation implications in natural resources management, agronomy, and agrochemical exposure risk assessments.

Key words: erosion—geographic information system (GIS)—length-slope (*LS*) factor—Natural Resources Inventory (NRI)—Revised Universal Soil Loss Equation (RUSLE)

Understanding the spatial variability of soil erosion at the watershed scale is an important component of many soil loss and soil conservation assessments. The Universal Soil Loss Equation (USLE) and its variations—Modified Universal Soil Loss Equation and Revised Universal Soil Loss Equation (RUSLE)—are commonly used to estimate soil loss due to runoff in watershed assessments. Both the USLE and the RUSLE equations are written as follows:

$$A = RKLSCP, \tag{1}$$

where A is the soil loss (t ha^{-1} y^{-1}); R is the rainfall erosivity factor (MJ mm ha^{-1} h^{-1} y^{-1}); K is the soil erodibility factor (t ha h [ha MJ mm]$^{-1}$); L is the slope length factor; S is the slope steepness factor; C is the cover management factor; and P is the supporting practice factor.

The L and S terms of the equation are often lumped together as *"LS"* and referred to as the topographic factor, which is considered to be more difficult to estimate than the other factors in the USLE equation (Wilson 1986). The advance of geographic information systems (GIS) has made it possible to use digital elevation models (DEM) to calculate *LS* factors across the landscape. Moore and Wilson (1992) presented a simplified equation for calculating the combined *LS*-factor over two-dimensional terrain. Their equation was shown to be equivalent to the RUSLE equations for the *LS*-factor (McCool et al. 1989) and was readily implemented in a GIS. Another approach presented by Desmet and Govers (1996) used upslope contributing area in calculating the slope length component of the *LS*-factor. They used a multiple-flow direction algorithm developed by Quinn et al. (1991) to calculate upslope contributing areas and applied that to the RUSLE *LS*-factor equations presented by McCool et al. (1987, 1989). Fu et al. (2006) adopted this same contributing area approach to *LS*-factor calculation in their application of the RUSLE and a sediment delivery model to evaluate the impacts of no-till practices on erosion and sediment yield. An additional important contribution of the work of Desmet and Govers (1996) was a method for dealing with complex catchments with multiple land uses. Their approach was to calculate upslope contributing areas independently for adjacent land uses that may be considered hydrologically independent. They proposed that surface runoff is rarely generated from an upland forest adjacent to a cultivated field and should not be considered as part of the upslope contributing area. Furthermore, they argued, land units are often separated by roads, ditches, or other drainage systems that isolate them hydrologically from their neighbors. Other methods have sought to address the potential shortcomings of the aforementioned approaches, such as accounting for areas of deposition on the landscape that impact slope length (Hickey 2000; Van Remortel et al. 2001). This approach explicitly addresses the deposition issues by evaluating changes in slope.

Much of the previous work described included some comparison of the computed values for *LS* with values obtained using other methods. Desmet and Govers (1996) compared the *LS* values calculated using their GIS-based approach with values obtained using the manual approach of Foster and Wischmeier (1974). They compared several different variations of the automated GIS method with the manual approach and determined that the GIS method generally predicted *LS* values 10% to 50% greater than the manual approach. They suggested that part of the reason for the high values obtained from the DEM method was because convergent flow was more realistically identified.

Michael F. Winchell is a senior GIS specialist at Stone Environmental Inc., Montpelier, Vermont. **Scott H. Jackson** is a principal scientist managing North American Free Trade Agreement regulatory strategy and stewardship at BASF Corporation, Research Triangle Park, North Carolina. **Adrian M. Wadley** is a senior research scientist at Stone Environmental Inc., San Francisco, California. **Raghavan Srinivasan** is director of the Spatial Sciences Laboratory, Department of Ecosystem and Science Management, Texas A&M University, College Station, Texas.

A study which compared several different GIS-based approaches to *LS* calculation was performed by Yitayew et al. (1999). They found that the average *LS* factor over a 4.5 ha (11.12 ac) watershed varied by as much as 100% depending upon the methodology employed. Yitayew et al. did not explicitly compare any of the GIS-based *LS* estimates with "ground-truth" values of *LS*. They did, however, compare the GIS-based erosion predictions using RUSLE with observed sediment yield in the watershed. Their findings showed that erosion was underpredicted by the GIS methods in high runoff years and overpredicted in low runoff years. Van Remortel et al. (2001) reported that the *LS* values generated using their approach agreed with recommended ranges for the RUSLE equation but that there had been no ground-truthing at the time of publication.

This paper builds upon previous work, making several modifications to previously presented *LS*-factor algorithms with a focus on the calculation of upslope contributing areas. A statistical comparison of the GIS-based *LS*-factors against field observations reported in the National Resources Inventory (NRI) database provides new evidence to support the applicability of GIS-based methods in capturing the spatial heterogeneity and magnitude of the *LS*-factor.

Materials and Methods

The procedure for a GIS-based approach to *LS*-factor calculation involves consideration of two key landscape characteristics: upslope contributing area and slope. While this study evaluates different algorithms for calculating slope, the emphasis is on the development of a method for computing upslope contributing areas.

Upslope Contributing Area. The form of the USLE topographic factor for a slope segment was shown by Foster and Wischmeier (1974) to be calculated as follows:

$$LS = \frac{S_j \times (\lambda_j^{m+1} - \lambda_{j-1}^{m+1})}{(\lambda_j - \lambda_{j-1}) \times (22.13)^m}, \qquad (2)$$

where L is the slope length factor for the jth segment; S_j is the slope factor for the jth segment; λ is the length from the lower boundary of the jth segment to the upslope boundary (m); and m is the length exponent of the USLE *LS*-factor.

Desmet and Govers (1996) derived an equation for the length component of the *LS*-factor for a two-dimensional surface. For use with a grid-based DEM, the equation is based on the upslope contributing area of each grid cell and may be written as follows:

$$L_{i,j} = S_{i,j}\,\frac{(A_{i,j-in} + D^2)^{m+1} - A_{i,j-in}^{m+1}}{D^{m+2} \times x_{i,j}^m \times (22.13)^m}, \qquad (3)$$

where $L_{i,j}$ is the L-factor for grid cell (i,j); $S_{i,j}$ is the slope factor for grid cell (i,j); $A_{i,j-in}$ is the contributing area at the inlet of a grid cell with coordinates (i,j) (m^2); D is the grid cell size (m); $x_{i,j}$ is the ($\sin\alpha i,j + \cos\alpha i,j$); $\alpha i,j$ is the aspect direction for the grid cell with coordinates (i,j); and m is the slope length exponent of the RUSLE *LS*-factor.

The most critical parameter to identify in equation three is the upslope contributing area. Computation of upslope contributing area can be based on either single-direction or multiple-direction flow algorithms. One disadvantage of the single-direction method is that it can only account for parallel or convergent flow. On complex topography, divergent flow can commonly occur, which can have a significant impact on upslope contributing area. Desmet and Govers (1996) concluded that a multiple-direction flow algorithm was the best approach for the development of an *LS* model and chose the algorithm developed by Quinn (1991) for their application. Tarboton (1997) developed an alternative multiple-direction flow algorithm for calculating upslope contributing area at each grid cell. Tarboton compared his multiple-direction flow algorithm (d-infinity) with a single-direction and several other multiple-direction flow algorithms, including the Quinn et al. (1991) method used by Desmet and Govers. Based upon statistical tests and examination of influence and dependence maps applied to difficult DEM surfaces, Tarboton suggested that his method performed as well or better than the other flow direction methods evaluated. For this reason and since the source code for Tarboton's method was readily available, the d-infinity method was adopted for this study.

Approaches to Constraining Upslope Contributing Area. One of the more challenging aspects of *LS*-factor models based on upslope contributing areas is how to account for landscape features that constrain contributing upslope area. The landscape features of interest are those that result in the termination of a continuous slope length. In the USLE, the theoretical terminus of a continuous slope length is the point at which soil deposition becomes dominant over erosion or gully erosion becomes dominant over sheet and rill erosion. Several landscape characteristics that are observable from GIS datasets may result in a zone of deposition. A change in slope leading to a concave surface is, perhaps, the landscape characteristic most explicitly related to deposition. This is a concept used by Hickey (2000) and Van Remortel et al. (2001) in their algorithm for calculating *LS*. The difficulty in this approach is in identifying the thresholds for changes in slope that indicate deposition. However, there are other directly observable landscape characteristics that we may use as surrogate indicators of deposition. These include residential/urban development, roads, stream channels, and land cover boundaries.

Features in urban and residential areas, including sidewalks, landscaping, curbs, drainage ditches, and stormwater systems physically alter the natural hydrologic flow paths of the landscape. Runoff flowing into a residential/urban area will tend to be diverted to a channelized flow system rather than following a natural flow path downslope. Based on this argument, we restricted the calculation of upslope contributing areas (and *LS*-factor) from continuous residential and urban land areas of greater than 1 ha (2.47 ac) as indicated by the nationally available, 30 m (98.4 ft) resolution National Land Cover Dataset (US Geological Survey [USGS] 1992).

In a similar way to residential/urban development, roads (ranging from interstate highways to farm roads) modify the natural hydrologic flow paths of the landscape. Both major roads and rural roads will have stormwater systems or drainage ditches that divert runoff to channelized flow systems or streams. These road features constrain the calculation of upslope contributing area by breaking the natural hill slope and transitioning sheet and rill erosion to gully erosion and concentrated flow. For this reason, we restricted the calculation of upslope contributing areas (and *LS*-factor) from road features based on the detailed roads data layer included in a national GIS dataset, ArcGIS 8.1 StreetMap (Environmental Systems Research [ESRI] 2001).

The calculation of a slope length for use in the RUSLE should terminate once a stream channel is encountered. For this application, we chose to use the DEM as the basis for identifying streams. We selected a drainage area threshold of 10 ha (24.71 ac), based on contributing area from a D-8 flow direction grid, to represent streams (a D-8 flow direction grid assumes that all flow from a source cell moves to a single adjacent cell). This threshold corresponded well to a vector dataset of streams (medium-resolution National Hydrography Dataset [USGS 1999a]) in a portion of our study area.

Land cover boundaries also have a critical impact on upslope contributing area calculation. This was discussed by Desmet and Govers (1996) and Van Oost et al. (2000). They proposed that when the landscape is considered as a single parcel of uniform land cover, unrealistically long slope lengths may be calculated based on the assumption that runoff is generated and available for sediment transport on all upslope areas. As previously discussed, this is often not the case, as certain land uses may not generate surface runoff, and many landscape units (such as cultivated fields) may be hydrologically isolated from their surroundings by drainage ditches and diversions. Furthermore, changes in vegetation that occur at boundaries of land cover units are frequently zones of soil deposition. This argument is made obvious by acknowledgement of the use of vegetated buffers to control the loss of soil, pesticides, and nutrients from downslope boundaries of agricultural fields. This study evaluates the calculation of *LS*-factors based on both the "single-parcel" assumption (i.e., the landscape is a homogeneous land cover) and the "multiple-parcel" assumption (i.e., the landscape is heterogeneous and processes occur at land cover boundaries that act to isolate parcels hydrologically and encourage zones of soil deposition). The presumption is that the single-parcel approach will result in a more "conservative" (higher) estimation of *LS*-factor values while the multiple-parcel approach will result in a more realistic but lower estimation of *LS*-factor.

As a final check against excessively long slope length calculations, all GIS approaches evaluated in this study imposed a cap of 333 m (1,000 ft) on slope lengths calculated from the DEM. Imposing this cap resulted in computed slope lengths of greater than 333 m being reduced down to the cap. The 333-m value was chosen based on recommendations by McCool et al. (1997) that a practical upper limit for slope lengths is around 333 m.

Slope Factor. There have been various suggestions in the literature regarding how to represent the slope-factor of the USLE/RUSLE in GIS-based calculations. Moore and Wilson (1992) proposed a simplified approach to the combined *L* and *S* factor. The WATEM program described in Van Oost et al. (2000) provided several options for calculating the slope component of *LS*, including the original equations developed by Wischmeier and Smith (1978), the RUSLE equations of McCool et al. (1989), an approach based on a power function of the slope gradient developed by Govers (1991), and a function developed by Nearing (1997). The RUSLE equations for the slope factor are used in the USDA RUSLE 2 program, which is considered by USDA to be the best available tool for predicting soil erosion. As such, the RUSLE methodology for slope factor calculation was adopted for this study. These equations are written as follows:

$$S = 10.8 \times \sin(b) + 0.03, \text{ where slope} < 9\%, \quad (4)$$
$$S = 16.8 \times \sin(b) - 0.50 \text{ where slope} \geq 9\%,$$

where *b* is the slope angle in radians.

Within a GIS, different algorithms are available for calculating slope at a grid cell. In this study, two different slope algorithms were evaluated. The first one is the ESRI method, which uses the eight surrounding cells to estimate the slope at a central cell based on a curve-fitting approach. This method assumes that the surface is continuous and differentiable and will tend to dampen the effects of anomalies within the DEM. The second slope algorithm evaluated was the TauDEM method. The TauDEM method calculates the slope based on the elevation difference between the central cell and the cell in the steepest downslope direction. This method may be more representative of a local slope but may tend to exaggerate slopes, especially where DEM anomalies exist.

Data Sources and Software. The calculation of the *LS*-factor required the following datasets. (1) DEM: The source for the DEM was the USGS Elevation Derivates for National Applications (USGS 2003). The data layer used from the Elevation Derivates for National Applications dataset was the 30-m (98.4 ft) resolution filled DEM. (2) Flow Accumulation: The Elevation Derivates For National Applications flow accumulation layer (based on a D-8 flow direction algorithm) was used for the identification of streams. (3) Land Cover: The 30-m resolution, 21-class National Land Cover Dataset 1992 (USGS 1999b) was used to identify the residential/urban areas as well as to distinguish landscape parcels in the multiple-parcel approach. (4) Roads: The ESRI ArcGIS StreetMap (ESRI 2001) vector roads dataset was used to represent roads for the study area. This vector layer was converted to a 30 m resolution raster dataset and used in the constraint of upslope contributing areas during calculation of the *LS*-factor.

A data processing script written using ArcObjects within ArcGIS 9.1 was used to generate the *LS*-factor datasets from the source datasets. In addition to the ESRI ArcObjects raster processing methods, the TauDEM 3.1 functions for calculating d-infinity flow direction, d-infinity flow accumulation, and d-infinity slope were used.

Results and Discussion

The approach presented in the previous section was applied to 40 agriculturally significant HUC4 watersheds in the central United States (figure 1). HUC4 is a term used to describe a 4-digit hydrologic unit defined by the USGS. Hydrologic units are a method used to define nested watersheds within the United States. The current method for accounting of watersheds includes 2-, 4-, 6-, 8-, 10-, and 12-digit hydrologic unit codes, with watersheds becoming progressively smaller as the number of digits in the hydrologic unit increases. There are 221 HUC4 watersheds in the United States. An example 30-m (98.4 ft) resolution *LS*-factor dataset is shown for HUC 0512 in figure 1.

Comparison of Length-Slope Factor Algorithms. The four GIS methods (single-parcel/ESRI slope, single-parcel/TauDEM slope, multiple-parcel ESRI slope, and multiple-parcel/TauDEM slope) were compared by calculating the percentiles of the *LS* values within each HUC8 in the study area. For each HUC8, the 5th, 10th, 25th, 50th, 75th, 90th, and 95th percentiles of *LS* for agricultural land covers were calculated. The analysis was restricted to agricultural land covers since those are the areas of greatest interest for the application of this dataset to agrochemical exposure assessments. Agricultural areas were identified from the National Land Cover Dataset. The National Land Cover Dataset land uses characterized as agricultural were orchard, pasture/hay, row

Figure 1

Analysis extent of 40 HUC4 watersheds and an example of a length-slope factor dataset calculated using the multiple-parcel ESRI slope algorithm approach.

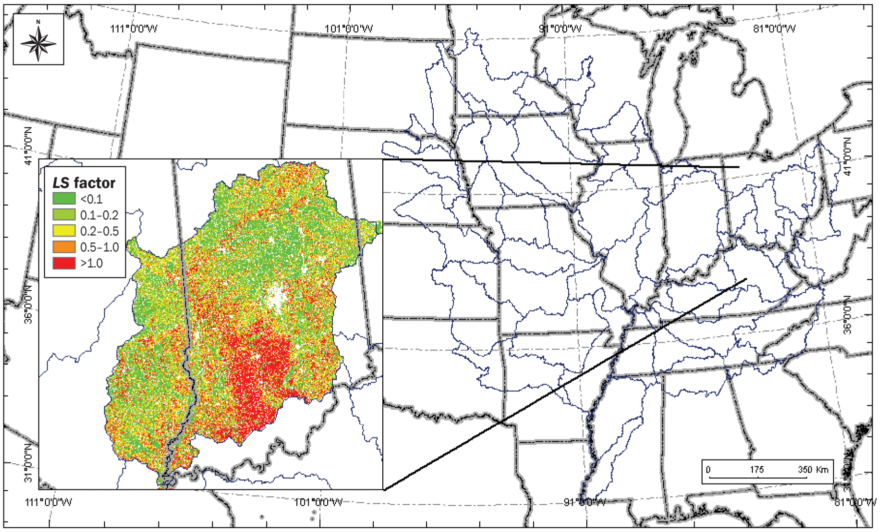

crop, small grains, and fallow. These statistics were calculated for 375 HUC8 watersheds within the study area. The mean and standard deviation of each percentile was then calculated for all the HUC8s for each of the four *LS* methods (table 1).

The results in table 1 show that the multiple-parcel methods result in lower *LS* values for all the percentiles, particularly for the higher percentiles. This is not unexpected and may be attributed to the longest slope length values associated with the single-parcel methods being more significantly constrained with the multiple-parcel approach. Smaller differences between the ESRI slope method results and the TauDEM slope method results are observed. In both the single-parcel and the multiple-parcel approaches, the TauDEM slope method results in a slightly broader distribution of *LS* values (greater extremes). This can be attributed to the greater smoothing of slopes that the ESRI algorithm produces as a result of its curve-fitting approach. Near the middle of the distributions (25th to 75th percentiles), the ESRI algorithm produces slightly lower *LS* values.

Comparison of Geographic Information System-Based Length-Slope Factor Values with Field Observations. An important objective of this study was to gain an understanding of how the GIS-based *LS*-factor values compare with those observed in the field. The dataset chosen to represent field observations was the NRI database (USDA NRCS 2000). The NRI database contains information on land use, soil characteristics, cropping practices, and erosion characteristics for sampling points throughout the United States. Included in the NRI database are input parameters to the USLE, including slope length and slope. While the precise location of the NRI sample points is confidential, the point locations may be approximated based on their HUC8, county, and Major Land Resource Area attributes. Within the 40 HUC4s that were evaluated for this study, there are 131,802 sample points in the NRI that include USLE attributes (based on the 1997 sampling). The number of points reported represents 375 of the 376 HUC8s within the 40 HUC4s evaluated. One HUC8 was not included due to processing constraints because of its size. All 131,802 points are on agricultural land uses. The number of sample points per HUC8 ranged from 8 to 1,567 with a median number of 287 points. While the NRI database provides an excellent statistical sample of *LS*-factors in a region, it is impossible for such a sample to capture the full range in conditions that can be found over such a large area.

For comparison with the GIS-based *LS*-factor values, percentiles of *LS* values within each HUC8 were calculated based on the NRI sample points. The NRI expansion factor (x-factor) associated with each sample point was used to weight each point appropriately. The x-factor describes the area in acres that the point represents. The same RUSLE-based equations used in the GIS-based method were used to calculate the *LS*-factor for the NRI points. For each HUC8, pairs of *LS* percentiles (GIS-based/NRI-based) were generated for the 5th, 10th, 25th, 50th, 75th, 90th, and 95th percentiles. These pairs of points were then plotted and regression equations were calculated to assess the relationship between the GIS and NRI methods. Points were plotted for only a single percentile on a graph (e.g., 50th, 90th) and for all percentile pairs plotted together. These pairs were generated for each of the four GIS-based *LS*-factor methods evaluated. Figures 2a through 2d show plots of the 50th percentile pairs plotted for the single-parcel/ESRI slope method, single-parcel/TauDEM slope method, multiple-parcel/ESRI slope method, and the multiple-parcel/TauDEM slope method respectively. In these plots, each point represents the 50th percentile GIS-based *LS* value versus NRI-based *LS* value for each of the 375 HUC8s evaluated. Figures 3a through

Table 1

Mean and standard deviation of HUC8 length-slope (*LS*) values by percentile for geographic information system-based *LS* methods.

	LS			
Percentile	**single parcel/ TauDEM slope**	**single parcel/ ESRI slope**	**multiple parcel/ TauDEM slope**	**multiple parcel/ ESRI slope**
5th	0.05 (0.06)	0.06 (0.07)	0.05 (0.05)	0.06 (0.07)
10th	0.11 (0.15)	0.13 (0.17)	0.10 (0.14)	0.12 (0.15)
25th	0.39 (0.57)	0.37 (0.53)	0.36 (0.48)	0.35 (0.46)
50th	1.03 (1.53)	0.98 (1.52)	0.90 (1.15)	0.85 (1.10)
75th	2.19 (3.04)	2.14 (3.15)	1.80 (1.99)	1.70 (1.93)
90th	3.95 (4.97)	3.92 (5.25)	3.08 (2.92)	2.93 (2.87)
95th	5.51 (6.43)	5.51 (6.85)	4.19 (3.63)	3.99 (3.61)

Note: Standard deviations are in parentheses.

Figure 2

Comparison of 50th percentile length-slope (*LS*) by HUC8 for (a) single-parcel method TauDEM slope algorithm, (b) single-parcel method ESRI slope algorithm, (c) multiple-parcel method, TauDEM slope algorithm, and (d) multiple-parcel method, ESRI slope algorithm.

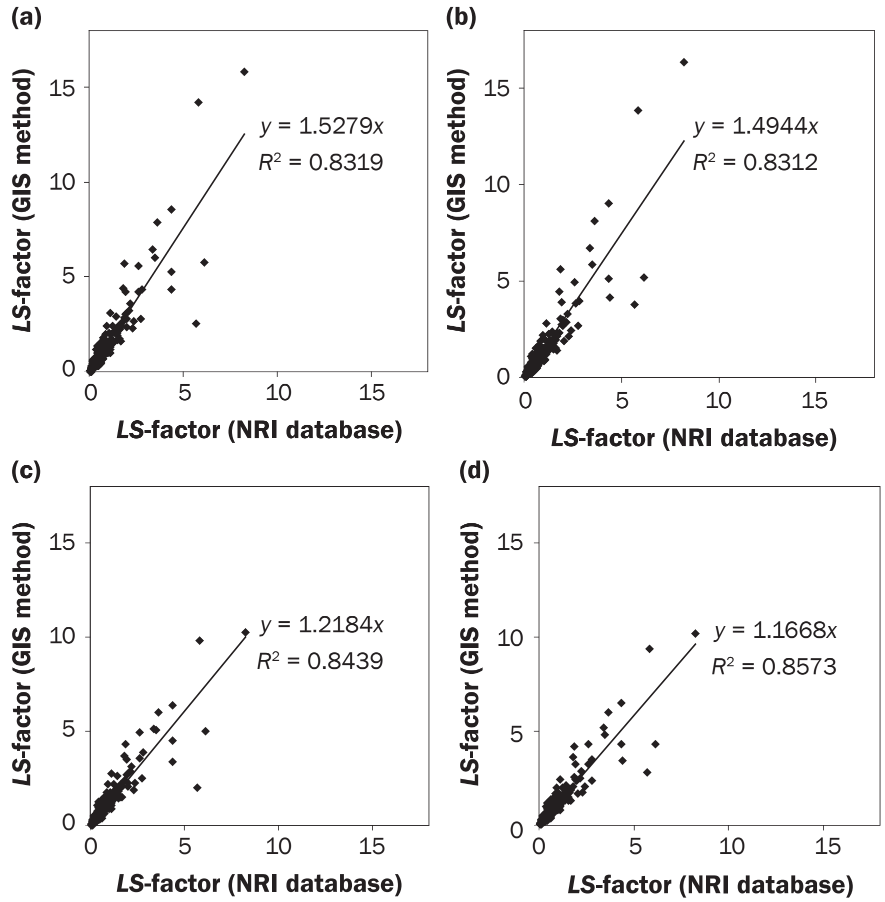

3d show the same plots for the 90th percentile *LS* values.

Reviewing figures 2 and 3 suggests several characteristics of the GIS-based method compared to the NRI method. First, r^2 values of the regressions range from 0.77 to 0.86, indicating that a strong correlation exists between the GIS-based *LS*-factors and the NRI-based *LS*-factors. Second, in all cases, the slope of the regression line (forced through a *y*-intercept of 0) is greater than 1.0, indicating that the GIS-based method results in higher estimates of the *LS*-factor than the NRI method. The single-parcel approaches result in a significantly higher bias in *LS*-factor values, with slopes in the 1.49 to 1.78 range, while the multiple-parcel approaches result in much less bias, with slopes in the 1.13 to 1.22 range. The data also suggests that the GIS-based methods have greater bias for the higher *LS* values (90th percentile) than the lower *LS* values (50th and all percentiles). The differences in fits between the GIS-based *LS* and the NRI-based *LS* values for the two different slope methods (ESRI and TauDEM) are less clear. We saw in table 1 that the TauDEM method results in slightly more extreme slope values and resulting higher *LS* values than the ESRI methods. However, data in table 2 suggests that the TauDEM slope method results in less bias than the ESRI method in 90th percentile *LS* factors for the single-parcel approach. The multiple-parcel results in table 2 corroborate the data in table 1, suggesting that the TauDEM slopes result in slightly higher bias in the 90th percentile *LS* factors.

An evaluation of the full distribution of *LS*-factor values for the GIS methods and the NRI database was performed for a large, agriculturally significant HUC8 in northwestern Illinois (HUC 07090005). Within this HUC8, there were 969 NRI sample points included in the construction of the distribution. The GIS methods each contained 4.8 million grid cells representing agricultural locations within the HUC8. The frequency distributions for each of the methods are shown plotted on figure 4. The multiple-parcel/ESRI slope method resulted in the closest agreement with the NRI distribution of *LS*-factor values, with a maximum difference between the 20th and 95th percentiles of around 20%. The shapes of the GIS-based and NRI-based distributions are remarkably similar, considering the differences in the sampling approaches and density. The particular HUC8 chosen was one that had a relatively high number of NRI points (969), suggesting that perhaps the "true" distribution of *LS*-factor values was more adequately sampled. Of the 375 HUC8s evaluated, 50% had fewer than 287 points. Low NRI sample density may be part of the reason for the differences in the *LS*-factors between the GIS approach and the NRI database.

Discussion. The comparison of the GIS-based *LS*-factors with the NRI database values produced encouraging results. There is clearly a strong correlation between the two sampling approaches; however, the *LS*-factor distribution based on the GIS methods consistently produced higher *LS* values. One factor contributing to the bias of the GIS methods is the significant differences between the sampling methods. In evaluating the GIS methods, every agricultural grid cell was considered a sample point, commonly resulting in millions of cells within a HUC8. The NRI database commonly contained only several hundred (median of 287) sample points within a HUC8. This difference in sampling density suggests that the GIS methods are more likely to be sampling the complete distribution of *LS*-factor values. This hypothesis was investigated by comparing the percentiles of the GIS-based and NRI-based *LS*-factors for only those HUC8s with greater sampling. The HUC8s that were in the top 25% in terms of both total sample points and sample point density (points per km^2) were evaluated independently. The 25th percentile for total sample points and point density were 478 points and 0.126 points km^{-2} respectively. The 25th percentile was chosen to capture HUC8s with significantly greater sampling than the median amount. Linear regression was performed for the *LS*-factor percentile

Figure 3

Comparison of 90th percentile length-slope (*LS*) by HUC8 for (a) single-parcel method TauDEM slope algorithm, (b) single-parcel method ESRI slope algorithm, (c) multiple-parcel method, TauDEM slope algorithm, and (d) multiple-parcel method, ESRI slope algorithm.

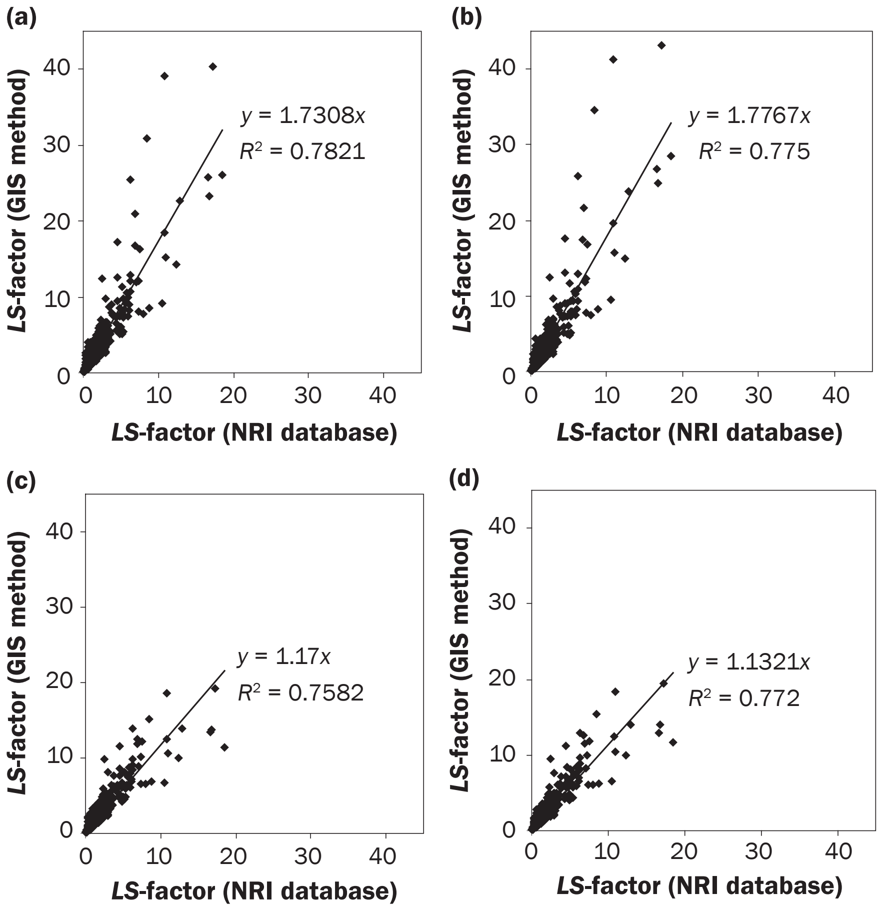

pairs for the 50th, 90th, and combined 5th to 95th percentiles for the multiple-parcel/ESRI slope method. The linear regression r^2 and regression line slope values for this evaluation are shown in table 2. When considering only HUC8s with greater sampling, the r^2 values improve for both the high point count and high point density cases, while the linear regression slope values only improve in the case of the high point count constraint on HUC8s. This brief investigation suggests that for HUC8s with greater NRI sampling, the distribution of *LS*-factor values estimated from the NRI points is more closely approximated by the GIS approach. This is not to say that the GIS-based method does not equally apply to HUC8s with smaller numbers of NRI sample points but rather that the GIS method is more strongly supported by the NRI database when the distribution of *LS* values is more comprehensively sampled by the NRI.

The preferred multiple-parcel GIS method for estimating *LS*-factors can be applied to any area where a suitable DEM and land use dataset exists (the approach applied in this study also incorporated a roads dataset). The method, which uses the contributing upslope area approach, has the potential to produce unrealistically long slope lengths for areas with infrequent changes in land cover and low road density, both of which act to constrain slope lengths. An alternative approach for identifying breaks in slope length involves the evaluation of change in slope, as proposed by Hickey (2000) and Van Remortel et al. (2001). Although more difficult to parameterize, this approach could provide improvements to the method presented and would likely result in lowering of some slope lengths and resulting *LS* values.

Summary and Conclusions

A GIS-based approach to generating high-resolution, spatially distributed *LS*-factor datasets for large watersheds was presented. The benefits in the approach developed include the incorporation of an infinite flow direction model (TauDEM) and additional methods for constraining slope lengths, including the use of roads and urban land use datasets. While the approach developed was not directly compared with others reported in the literature, it may be considered as a further refinement of the Desmet and Govers (1996) method that should be applied in situations where complex topography may be influencing overland flow paths and where excessively long slope lengths calculated from a DEM may require further constraint based on landscape features. The greatest limitation of this method is the absence of an algorithm for predicting topographically-driven zones of soil deposition.

Several variations of the GIS approach were compared, including single-parcel and multiple-parcel methods and variations on the slope calculation algorithm (ESRI and TauDEM methods). The ESRI slope algorithm method was preferred because it considers the broader slope of the landscape by evaluating all neighboring grid cells and is less prone to extreme slope values. The multiple-parcel approach was preferred over the single-parcel approach, since it more effectively constrains slope lengths.

The GIS *LS*-factor results were compared with field-based assessments of *LS*-factors reported in the NRI database by evaluating the percentiles from their statistical distributions at the HUC8 level. The comparisons showed that the multiple-parcel/ESRI slope method produced the closest approximation to the NRI data distributions; however, all GIS methods had a positive bias. The fit between the GIS and NRI *LS*-factors improved somewhat when considering only HUC8s that been more extensively sampled in the NRI database.

The approach presented in this study was applied to a large section of the Mississippi River watershed and may be extended to other regions with suitable datasets. The value of a spatially explicit *LS*-factor dataset for use in soil conservation applications is fully realized when incorporated in an automated process to predict spatially explicit soil loss and sediment yield estimates (Fernandez et al. 2003; Fu et al. 2006). Given the importance of the *LS*-factor in GIS-based methods for soil erosion calculations, further refinement and validation of

Table 2
The r^2 value and trend line slope values for linear regression of National Resources Inventory-based length-slope (*LS*) percentiles vs. geographic information system–based *LS* percentiles by HUC8.

Percentile	Single parcel/ TauDEM slope	Single parcel/ ESRI slope	Multiple parcel/ TauDEM slope	Multiple parcel/ ESRI slope	Multiple parcel/ ESRI slope (high point count*)	Multiple parcel/ ESRI slope (high point density†)
50th	0.83 (1.53)	0.83 (1.49)	0.84 (1.22)	0.86 (1.17)	0.86 (1.05)	0.87 (1.16)
90th	0.78 (1.73)	0.78 (1.78)	0.76 (1.17)	0.77 (1.13)	0.82 (1.08)	0.85 (1.15)
All	0.84 (1.73)	0.83 (1.78)	0.85 (1.18)	0.85 (1.14)	0.91 (1.10)	0.92 (1.16)

Note: Trend line slope values are in parentheses.

* High point count includes only HUC8 watersheds with a total number of NRI sample points in the upper 25% of all HUC8s evaluated (478 points).

† High point density includes only HUC watersheds with a point density (NRI points per square km) in the upper 25% of all HUC8s evaluated (0.126 points km^{-2}).

Figure 4
Comparison of length-slope (*LS*) factor frequency distributions, HUC 07090005.

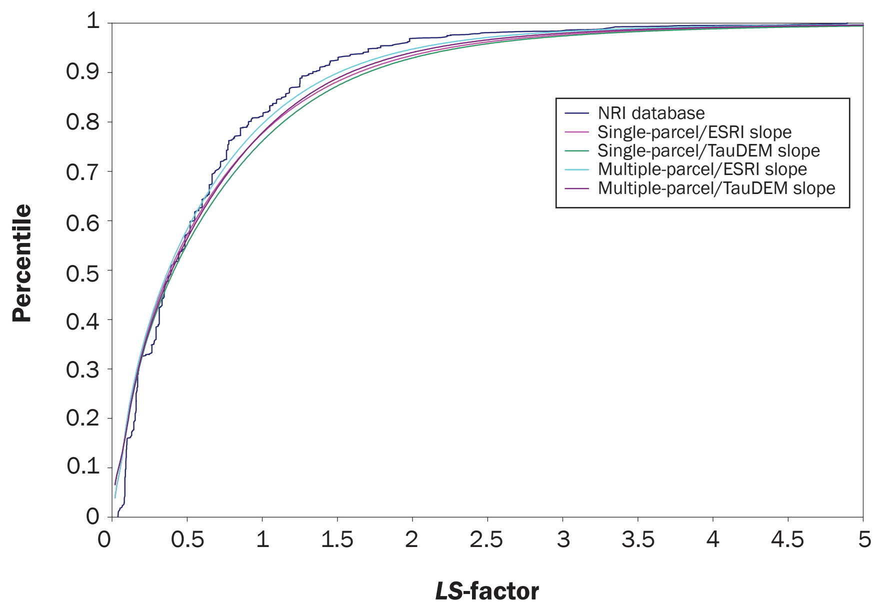

LS-factor algorithms are needed. In particular, techniques that use breaks in slope identified from the DEM to locate soil deposition zones, such as the approach of Van Remortel et al. (2001), should be further investigated along with new approaches to constraining slope lengths to reasonable values. Finally, while this study used a statistical sample of *LS*-factors to validate the GIS-method at a large watershed scale, site-specific validation of GIS-based values with field measurements of *LS* would be invaluable.

Acknowledgements

This research was funded in part by BASF Corporation, Crop Life America, and Syngenta Crop Protection. The authors recognize valuable input from Tharacad Ramanarayanan (Bayer CropScience), Pat Havens (Dow AgroSciences), and Paul Hendley (Syngenta Crop Protection).

References

Desmet, P.J.J., and G. Govers. 1996. A GIS procedure for automatically calculating the USLE LS-factor on topographically complex landscape units. Journal of Soil and Water Conservation 51(5):427-433.

ESRI (Environmental Systems Research Inc.). 2001. StreetMap USA. Redlands, CA: ESRI.

Fernandez, C., J.Q. Wu, D.K. McCool, and C.O. Stockle. 2003. Estimating water erosion and sediment yield with GIS, RUSLE, and SEDD. Journal of Soil and Water Conservation 58(3):128-136.

Foster, G.R., and W.H. Wischmeier. 1974. Evaluating irregular slopes for soil loss prediction. Transactions of ASAE 17(1):305-309.

Fu, G.B., S.L. Chen, and D.K. McCool. 2006. Modeling the impacts of no-till practice on soil erosion and sediment yield with RUSLE, SEDD, and ArcView GIS. Soil and Tillage Research 85(2):38-49.

Govers, G. 1991. Rill erosion on arable land in Central Belgium: Rates, controls and predictability. Catena 18(2):133-155.

Hickey, R. 2000. Slope angle and slope length solutions for GIS. Cartography 29(1):1-8.

McCool, D.K., L.C. Brown, G.R. Foster, C.K. Mutchler, and L.D. Meyer. 1987. Revised slope steepness factor for the Universal Soil Loss Equation. Transactions of ASAE 30(5):1387-1396.

McCool, D.K., G.R. Foster, C.K. Mutchler, and L.D. Meyer. 1989. Revised slope length factor for the Universal Soil Loss Equation. Transactions of ASAE 32(5):1571-1576.

McCool, D.K., G.R. Foster, and G.A. Weesies. 1997. Slope-length and steepness factors (LS). *In* Predicting Soil Erosion by Water: A Guide to Conservation Planning with the Revised Universal Soil Loss Equation (RUSLE). USDA Agriculture Handbook No. 703, Chapter 4. Washington, DC: USDA.

Moore, I.D., and J.P. Wilson. 1992. Length-slope factors for the Revised Universal Soil Loss Equation: Simplified method of estimation. Journal of Soil and Water Conservation 47(5):423-428.

Nearing, M.A. 1997. A single continuous function for slope steepness influence on soil loss. Soil Science Society of America Journal 61:917-919.

Quinn, P.F., K.J. Beven, P. Chevallier, and O. Planchon. 1991. The prediction of hillslope flow paths for distributed hydrological modeling using digital terrain models. Hydrological Processes 5(1):59-79.

Tarboton, D.G. 1997. A new method for the determination of flow directions and contributing areas in grid digital elevation models. Water Resources Research 33(2):309-319.

USDA Natural Resource Conservation Service (NRCS). 2000. 1997 National Resources Inventory (NRI) Database. Washington, DC: USDA NRCS.

USGS (US Geological Survey). 1999a. National Hydrography Dataset (NHD): Medium resolution. Reston, VA: USGS.

USGS. 1999b. National Land Cover Dataset 1992. Sioux Falls, SD: USGS.

USGS. 2003. Elevation Derivatives for National Applications (EDNA). Sioux Falls, SD: USGS.

Van Oost, K., G. Govers, and P. Desmet. 2000. Evaluating the effects of changes in landscape structure on soil erosion by water and tillage. Landscape Ecology 15(6):577-589.

Van Remortel, R., M. Hamilton, and R. Hickey. 2001. Estimating the LS factor for RUSLE through iterative slope length processing of digital elevation data. Cartography 30(1):27-35.

Wischmeier, W.H., and D.D. Smith. 1978. Predicting Rainfall Erosion Losses: A Guide to Conservation Planning. USDA Agricultural Handbook 537. Washington, DC: USDA.

Wilson, J.P. 1986. Estimating the topographic factor in the universal soil loss equation for watersheds. Journal of Soil and Water Conservation 41(3):179-184.

Yitayew, M., S.J. Pokrzywka, and K.G. Renard. 1999. Using GIS for facilitating erosion estimation. Applied Engineering in Agriculture 15(4):295-301.